SPECTRAL ANALYSIS OF NOISY OSCILLATORS NEAR HOPF BIFURCATIONS*

I.A. Khovanov[a,b], L. Schimansky-Geier[b], M.A. Zaks[b]

[a]Department of Physics, Lancaster University
Lancaster LA1 4YB, United Kingdom
[b]Institute of Physics, Humboldt-University at Berlin
Newtonstr. 15, D-12489 Berlin, FR Germany

(Received February 21, 2006)

We compare the dynamics of nonlinear noisy oscillators near the two types of the Hopf bifurcation. Prior to the bifurcation, in the regime of damped oscillations around the stable focus, noise serves as a bifurcation precursor: the power spectrum includes a peak at the frequency of the self-sustained oscillations. Super- and sub-critical Hopf bifurcations differ crucially in the noise dependence of the width of this spectral line. In case of a super-critical bifurcation the width is a monotonically growing function of the noise intensity. In contrast, for a sub-critical bifurcation, growth of the intensity of the weak noise enforces a decrease of the peak width; the width starts to grow only when the noise level exceeds a certain threshold value. Since the inverse spectral width is a measure of coherence, we conclude that true noise-induced coherence can be found only near the sub-critical bifurcation.

PACS numbers: 05.40.Ca, 05.45.–a, 42.65.Sf

1. Introduction

For obvious fundamental and practical reasons, complicated interplay of stochastics and dynamics near the onset of oscillations remains a highly relevant topic [1–5]. Implications of noise affect dynamical aspects of many phenomena in physics, chemistry and biology, from mechanisms behind the climatic variability [6] to distinction of frequencies in mammalian auditory systems [7,8]. The constructive role of noise is well seen in the phenomenon of coherence resonance (CR) [9–11]: at a certain, finite noise level the noise-induced oscillations attain a maximum degree of coherence.

* Presented at the XVIII Marian Smoluchowski Symposium on Statistical Physics, Zakopane, Poland, September 3–6, 2005.

CR is enrooted in the interaction between nonlinearity and noise. Especially well this interaction has been examined theoretically and verified in experiments for excitable systems [10, 11]: systems with stable steady states, finite perturbation thresholds for "firing", and refractory periods during which they do not respond to perturbations. Under the action of noise, such systems display quasi-regular spiking sequences; an adequate theory of this effect neglects the amplitude fluctuations and reduces the description to simple phase dynamics [12].

Another context in which CR plays an important role is the influence of noise upon dynamics close to bifurcations. Here, noise manifests itself in the form of "precursors" of bifurcations: additional peaks in the power spectra. At a certain noise intensity such precursors become especially distinct; this is often interpreted as increase in coherence. Numerically, this phenomenon has been studied for the period-doubling bifurcation and the torus birth [13]. Close to the onset of a super-critical Hopf bifurcation, resonance-like behavior has been recovered in computer simulations [14–17], detected in experiments on plasma waves [18, 19] and electro-chemical reactions with nickel and platinum [20]. Recently, CR in a semiconductor laser near the Hopf bifurcations has been experimentally investigated in [21], where noise-induced resonances occur for both the sub- and super-critical bifurcation type. However, the specific response has been found to depend crucially on the character of the bifurcation.

Below, we examine systematically the prototype case of the Hopf bifurcation: the super- and the sub-critical one, and check whether one can indeed speak about the improvement of coherence. Analysis of the noisy dynamics in a simple canonical model discloses qualitative differences between the two types of the bifurcation. Theoretical conclusions well match the results of the numerical simulation and display a remarkable correspondence with the experimental data.

2. Dynamical model and its power spectra

Onset and enhancement of self-sustained oscillations can be successfully modeled by the complex differential equation

$$\dot{z} = -i\omega_0 z + zF(z)\,, \tag{1}$$

used in many different contexts, *e.g.* to describe a self-sustained oscillator in laser in the rotating wave approximation [22]. Here $z = x + iy$ is a complex amplitude, ω_0 is the eigenfrequency. In fact, the model (1) is a normal form for the Andronov–Hopf bifurcation, obtained from a generic dynamical system near the bifurcation point by standard reduction technique (see [23] for details); examples of applications range from the Van der Pol equation

to the Lang–Kobayashi mean field equations with delay for lasers. The bifurcation scenario depends on the non-linear function $F(z)$. For the super-critical Hopf bifurcation, $F(z)$ takes the form

$$F(z) = F_1(r) = a_1 - r^2 \tag{2}$$

with $r = |z| = \sqrt{x^2 + y^2}$; at $a_1 = 0$ the equilibrium at $|z| = 0$ gets destabilized, and the stable limit cycle is born from it. Alternatively, the sub-critical Hopf bifurcation is rendered by

$$F(z) = F_2(r) = a_2 + r^2 - r^4 \,. \tag{3}$$

Here, the increase of the parameter a_2 results, first, in the birth of the finite-amplitude oscillatory state at $a_2 = -1/4$ and, second, in the destabilization of equilibrium at $a_2 = 0$. The former event is the saddle-node (tangent) bifurcation which creates on the phase plane two limit cycles: the stable and the unstable one. The latter event is the Hopf bifurcation: the unstable limit cycle shrinks to the equilibrium which, thereafter, inherits its instability. In the parameter range between two bifurcations the system has two attractors: the equilibrium and the stable limit cycle.

Certain experimental systems can be tuned close to a state in which the branching coefficient vanishes and the onset of oscillatory mode changes from super- to sub-critical; this behavior was reported *e.g.* for semiconductor lasers with active feedback [24]. While modeling such situations, both of the above types of nonlinearities should be treated[1].

Below, we set $\omega_0 = 1$ and fix the values $a_1 = -0.01$ and $a_2 = -0.3$, respectively. This choice adjusts the system before the birth of self-sustained oscillations, $z = 0$ being a stable fixed point and $dr/dt < 0$ everywhere outside this point. The latter inequality rules out excitability, since the amplitude of any perturbation monotonically decays. Note that a reduced phase description is not sufficient in the present case, and the full amplitude dynamics has to be treated.

In the presence of noise the model turns into:

$$\dot{z} = -i\omega_0 z + zF(z) + \sqrt{2D}\xi(t) \,, \tag{4}$$

here $\xi(t) = \xi_x(t) + i\xi_y(t)$ represents a complex white noise source with intensity D and two independent components.

Though of general nature, the model (4) accounts, in particular, for the essential features of a laser. Recently this has allowed us to relate our results to experimental findings [21]. In the first operation point a stable

[1] Qualitatively, both scenarios can be unified within a single two-parameter description; for our current purposes, their separate treatment is sufficient.

focus "almost" gives birth to a limit cycle, whereas, in the second case the laser is close to a saddle-node bifurcation of periodic states, after which a stable fixed point and a stable limit cycle coexist.

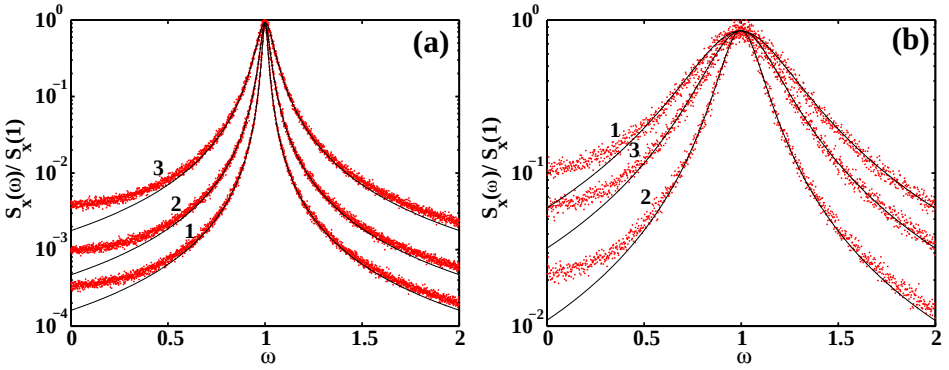

Fig. 1. Power spectra $S_x(\omega)$ for different levels of noise. Data are normalized to their maximal values. Dots: experimental points, solid lines: Lorentzian fits. (a) Super-critical bifurcation. Curves: 1 — noise intensity beneath maximum of β, 2 — maximum of β, 3 — beyond maximal value of β. (b) sub-critical bifurcation. Curves: 1 — noise intensity beneath minimum of width Δ_ω, 2 — minimum of Δ_ω, 3 — beyond minimal value of Δ_ω.

In a noisy experimental setup, a precursor of the bifurcation manifests itself as a noise-induced peak in the power spectrum of system response. In the experimental data, the peaks in the power spectra were fitted through Lorentzian line-shape function [21]. Several typical power spectra for numerically computed trajectories of (4) are presented in Fig. 1. The computed power spectra are also fitted by Lorentzian functions. Note, that these functions approximate the noise-induced spectral peak quite accurately.

The quantitative characteristics of the spectral response are the peak frequency ω_{P}, the full width at half maximum $2\Delta_\omega$, and the peak height H. The Fourier transformation translates the width Δ_ω into the correlation time $\tau_{\mathrm{c}} \sim 1/\Delta_\omega$. The quality factor $Q = \omega_P/\Delta_\omega$ is an inverse function of the width. A measure characterizing the noise-induced response is the signal-to-noise ratio [9, 11, 13]

$$\beta = HQ = \frac{H\omega_P}{\Delta_\omega}\,. \tag{5}$$

Spectral characteristics obtained from numerical simulation of (4) are summarized in Fig. 2. Resonance-type response is found for both kinds of bi-

furcation and, even more strikingly, width and peak height exhibit the same qualitative behavior for the sub- and super-critical type as observed in the experiment.

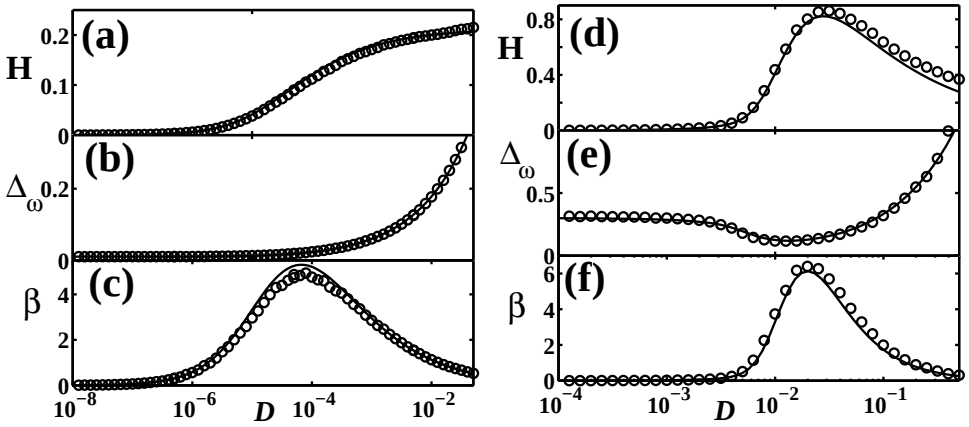

Fig. 2. Peak height H, width Δ_ω, and signal-to-noise ratio β *versus* noise intensity D. Left column: super-critical bifurcation, $F = F_1$. Right column: sub-critical bifurcation, $F = F_2$. Empty circles represent the results of numerical simulations of (4), curves are obtained from the analytical treatment.

3. Explicit estimates and discussion

Some more insight into the nature of the observed effects can be obtained by analytical treatment. Rewritten in terms of the variable $w = u + iv = z\exp(i\omega_0 t)$, Eq. (4) turns into

$$\dot{w} = wF(w) + \sqrt{2D}\xi_w(t)\,, \tag{6}$$

where the noise $\xi_w(t)$ shares the properties with $\xi(t)$. The spectrum S of the variable x (or y) at $\omega > 0$ is related to the spectrum of the variable u (or v) by $S_x(\omega) = S_u(\omega + \omega_0)/2$. Experimental and numerical data suggest usage of the Lorentzian ansatz

$$S_u(\omega) = \frac{2D}{\pi(\Delta_\omega^2 + \omega^2)}\,. \tag{7}$$

For this parameterization, width and peak height are interrelated by $H = 2D/(\pi\Delta_\omega^2)$. The width is determined by the Parseval theorem, which

provides in combination with a Lorentzian spectrum

$$\int_{-\infty}^{\infty} S_u(\omega)d\omega = \frac{2D}{\Delta_\omega} = \langle u^2 \rangle = \frac{\langle r^2 \rangle}{2}\,,$$

hence

$$\Delta_\omega \;=\; 2\frac{D}{\langle r^2 \rangle}\,, \tag{8}$$

$$\langle r^2 \rangle \;=\; \int_0^{\infty} r^2 P(r)dr\,. \tag{9}$$

The amplitude r has a Rayleigh-like distribution [1, 22]

$$P(r) = Nr\exp\left(-\frac{U(r)}{D}\right), \tag{10}$$

N being a normalization constant. The potential $U(r) = -\int rF(r)dr$ is given by $U_1(r) = -a_1 r^2/2 + r^4/4$ for the super-critical bifurcation and by $U_2(r) = -a_2 r^2/2 - r^4/4 + r^6/6$ for the sub-critical case. For $U_1(r)$, the integral (9) can be written explicitly in terms of exponential and error functions:

$$\Delta_\omega^{(1)} = \frac{2}{\frac{\exp\left(-a_1^2/8D\right)}{\sqrt{D\pi}\left[1-\mathrm{erf}(-a_1/\sqrt{8D})\right]} + \frac{a_1}{2D}}\,. \tag{11}$$

In the relevant range of D, a sufficiently accurate approximation for the spectral width is

$$\Delta_\omega^{(1)} \cong -\frac{a_1}{2} + \frac{\sqrt{a_1^2 + 12D}}{2}\,. \tag{12}$$

Accordingly, $\Delta_\omega^{(1)}$ stays practically constant for small noise and increases as $\sqrt{D}$ at larger D (Fig. 2(a)). The peak height, on the other hand, grows initially like $H \sim D$ and saturates for stronger noise (Fig. 2(b)). This behavior of the width and the height results in a maximum of β at certain D (Fig. 2(c)).

In the sub-critical case, the integral (9) has to be evaluated numerically. Since the maximum of the distribution (10) shifts to larger r with the growth of D, the level of noise determines the range of the function $U_2(r)$ which makes the crucial contribution into the integral. For small noise levels, the term $\sim r^2$ dominates and, consequently, $\Delta_\omega^{(2)}$ is nearly constant as

in the super-critical case. For moderate noise, the second term acquires importance, and the potential becomes almost a linear function $U_2 \sim r$ so that $\Delta_\omega^{(2)} \sim D^{-1}$ decreases when the noise grows. Eventually, the third term in U_2 takes over, producing again an increase $\Delta_\omega^{(2)} \sim D^{2/3}$. In this way, the spectral width turns out to be a non-monotonic function with a distinct minimum at certain noise level. The correlation time of the system in this case possesses a maximum. This manifestation of coherence resonance reminds the system response for the excitable CR [10], with an important distinction: here the noise-induced peak appears at infinitely small noise level, whereas at CR in an excitable system it requires a finite noise intensity, that leads to a sharp transformation of the spectrum.

Apparently, this effect is not restricted to the particular form of F_2 used above. Its mechanism — competition between the destabilizing term $\sim r^2$ and a higher-order stabilizing term — is generic for sub-critical bifurcations.

We explain the differences between super- and sub-critical cases by the following arguments. First, we note that the damping of (4), function $F(r)$, is related to the value of the second derivative of the amplitude potential:

$$\frac{d^2U(r)}{dr^2} = -F(r) - r\frac{dF}{dr}; \tag{13}$$

locally, $d^2U(r)/dr^2$ defines a relaxation time of the system (4). Second, since the amplitude r is distributed according to (10), its mean value $\langle r \rangle$, as a function of D, moves from small to large values when the noise becomes stronger (see Fig. 5). In other words, for different intensities of noise, oscillations occur in regions with different local curvature of the potential $U(r)$.

For super-critical case $d^2U(r)/dr^2$ is a monotonically increasing function of r and, consequently, of the noise intensity D. In the region of weak noise, it almost does not grow, and we observe noise-induced oscillations with larger amplitude and nearly the same coherence properties (compare Fig. 3(a) and (b)). This can be related to phase dynamics via the number and statistics of the zero-crossings of the trajectory. After $d^2U(r)/dr^2$ is noticeably increased, the coherence gets lost (Fig. 3(c)), *i.e.* zero-crossings become rather disordered.

For sub-critical case the damping $d^2U(r)/dr^2$ is a non-monotonic function of r: in the range of moderate amplitude r it is decreasing. Accordingly, when the trajectory of the system visits the region with low damping, we observe time intervals of oscillations with high coherence (compare Fig. 4 (a) and (b)). For large noise intensity, $d^2U(r)/dr^2$ is significantly increased, and coherent oscillations do not occur.

Nonlinearity in the amplitude equation is related to nonlinearity in damping. Before the super-critical Hopf bifurcation the damping is minimal in the

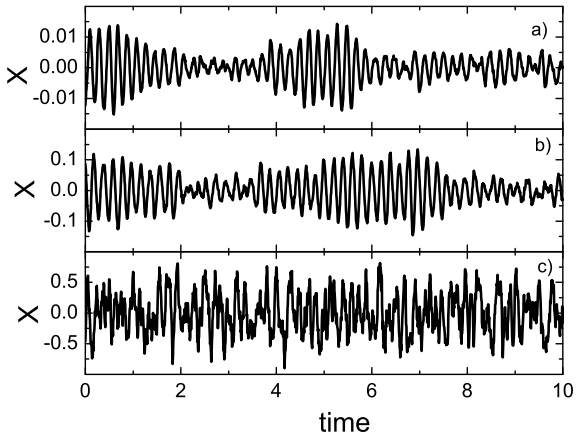

Fig. 3. Numerical trajectories for different levels of noise in the case of super-critical bifurcation. Panel (a) corresponds to noise intensity beneath the maximum of β, (b) — maximum of β, (c) — beyond maximal value of β.

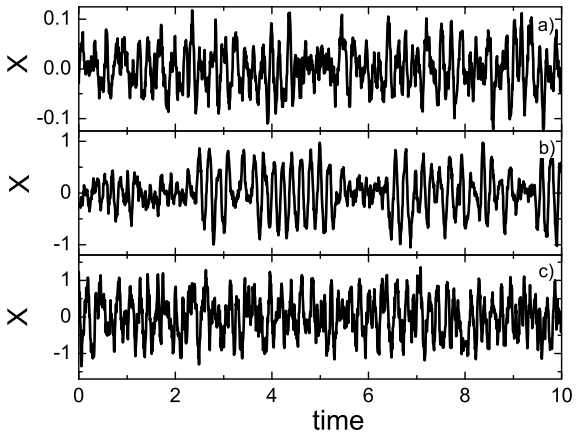

Fig. 4. Numerical trajectories for different level of noise in the case of sub-critical bifurcation. Panel (a) corresponds to noise intensity beneath minimum of the width Δ_ω, (b) — minimum of Δ_ω, (c) — beyond minimal value of Δ_ω.

fixed point, whereas before the sub-critical bifurcation the minimal damping values take place outside the fixed point, in the region where a limit cycle arises. Consequently, the main ingredient for the differences between the manifestations of CR is the difference in the form of dependence of damping on the coordinate. It means, that similar effects can be observed in

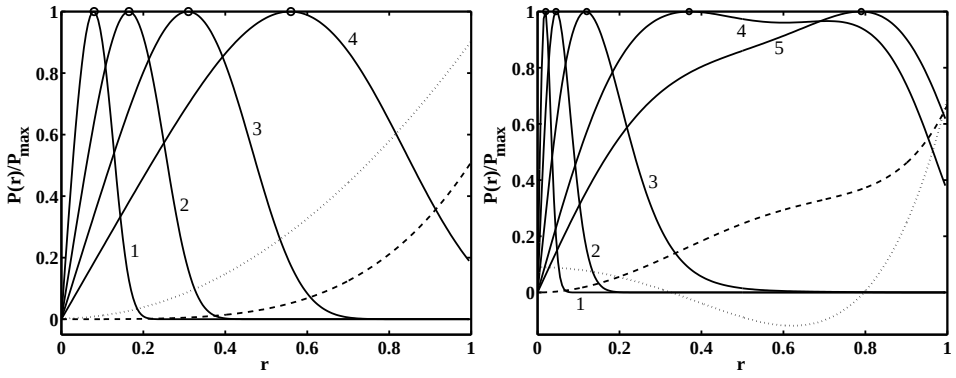

Fig. 5. Normalized distribution $P(r)$ for different levels of noise. Left panel: super-critical case. Solid curves: 1 — D=0.0001, 2 — D=0.001, 3 — D=0.01, 4 — D=0.1. Right panel: sub-critical case. Solid curves: 1 — D=0.0001, 2 — D=0.0006, 3 — D=0.004, 4 — D=0.025, 5 — D=0.04. Dashed lines: shapes of potentials $U_{1,2}(r)$ (arb. units). Dotted lines: profiles of $d^2U_{1,2}/dr^2$ (arb. units). Maxima of distributions are marked by circles.

oscillators with particular form of nonlinear damping term, whereby such oscillators may not demonstrate bifurcations and regimes of self-oscillations.

In conclusion, we have demonstrated that resonance phenomena driven by noise are general concomitant features of a Hopf bifurcation. However, while the existence of an optimum noise level is a common feature for both types of bifurcations, the physics behind the resonance effect is qualitatively different. In the super-critical case, the increase of the signal-to-noise ratio is produced by the spectral peak height, that is by an increase of the oscillation amplitude. The width is initially only slightly affected, but increases steeply for stronger noise, weakening the coherence. Resonance-like behavior originates from the competition between the growth rates for the height and the width. In contrast, for the sub-critical type, the spectral width itself exhibits a minimum. Here, the noise improves indeed the quality factor as well as the temporal coherence of the oscillatory transients. In a strict sense, only this kind of response should be termed "coherence resonance". These qualitative differences between the sub- and super-critical case are related to amplitude dynamics, whereas the effect of noise on the frequencies is insignificant. The degree of coherence depends on the effective damping, determined by the local value of $d^2U(r)/dr^2$ at the maximum of the amplitude distribution. Growth of the noise shifts this maximum towards larger r. In the super-critical case, the damping is a monotonic function of the amplitude and, hence, of the noise. The sub-critical case is distinguished

by a non-monotonic relation between the local slope of the potential and the noise intensity. Accordingly, in a certain intermediate range of noise, weakly damped coherent oscillations with moderate amplitudes are excited.

This work was partly supported by the Collaborative Research Center "Complex Nonlinear Processes" of German Science Foundation (DFG-Sfb555) and Alexander-von-Humboldt Foundation (I.Kh.). We thank F. Henneberger, H.-G. Wünsche and O. Ushakov for fruitful cooperation.

REFERENCES

[1] H. Risken. *Fokker-Planck Equation*, Springer, Berlin 1984.
[2] D. Ryter, P. Talkner, P. Hänggi, *Phys. Lett.* **A93**, 447 (1983).
[3] P. Talkner, P. Hänggi, *Phys. Rev.* **A29**, 768 (1984).
[4] P. Hänggi, M. Borkovec, P. Talkner, *Rev. Mod. Phys.* **62**, 251 (1990).
[5] R. Rozenfeld, J. Łuczka, P. Talkner, *Phys. Lett.* **A249**, 409 (1998).
[6] A. Ganopolski, S. Rahmstorf, *Phys. Rev. Lett.* **88**, 038501 (2002).
[7] T. Risley, J. Prost, F. Jülicher, *Phys. Rev. Lett.* **93**, 175702 (2004).
[8] R. Stoop, A. Kern, *Phys. Rev. Lett.* **93**, 268103 (2004).
[9] Hu Gang *et al.*, *Phys. Rev. Lett.* **71**, 807 (1993).
[10] A. Pikovsky, J. Kurths, *Phys. Rev. Lett.* **78**, 775 (1997).
[11] B. Lindner, J. Garcia-Ojalvo, A. Neiman, L. Schimansky-Geier, *Phys. Rep.* **392**, 321 (2004).
[12] B. Lindner, A. Longtin, L. Schimansky-Geier, *Phys. Rev.* **E66**, 031916 (2002).
[13] A. Neiman, P.I. Saparin, L. Stone, *Phys. Rev.* **E56**, 270 (1997).
[14] Z. Hou, H. Xin, *Phys. Rev.* **E60**, 6329 (1999); W. Ebeling, H. Herzel, W. Richert, L. Schimansky-Geier, *ZAMM* **66**, 141 (1986).
[15] S. Katsev, I.L. Heureux, *Phys. Rev.* **E61**, 4972 (2000).
[16] A.F. Rozenfeld, C.J. Tessone, E. Albano, H.S. Wio, *Phys. Lett.* **A280**, 45 (2001)
[17] G.S. Jeon, M.Y. Choi, *Phys. Rev.* **B66**, 064514 (2002).
[18] L. I, J.-M. Liu, *Phys. Rev. Lett.* **74**, 3161 (1995).
[19] A. Dinklage, C. Wilke, T. Klinger, *Phys. Plasmas* **6**, 2968 (1999).
[20] I.Z. Kiss, J.L. Hudson, G.J.E. Santos, P. Parmananda, *Phys. Rev.* **E67**, 035201(R) (2003).
[21] O. Ushakov, H.-J. Wünsche, F. Henneberger, I.A. Khovanov, L. Schimansky-Geier, M.A. Zaks, *Phys. Rev. Lett.* **95**, 123903 (2005).
[22] R.D. Hempstead, M. Lax, *Phys. Rev.* **161**, 350 (1967).
[23] Y.A. Kuznetsov, *Elements of Applied Bifurcation Theory*, Springer-Verlag, New-York, Berlin, Heidelberg 1998.
[24] S. Bauer, O. Brox, J. Kreissl, B. Sartorius, M. Radziunas, J. Sieber, H.-J. Wünsche, F. Henneberger, *Phys. Rev.* **E69**, 016206 (2004).